Enhancement of positron binding energy in molecules containing π bonds

J. R. Danielson,* S. Ghosh, and C. M. Surko
Physics Department, University of California San Diego, La Jolla, CA 92093, USA
(Dated: August 8, 2022)

Observation of vibrational Feshbach resonances (VFR) in the annihilation spectra of positrons on molecules provides a direct measurement of the positron-molecule binding energy ε_B. New annihilation measurements are presented for ring hydrocarbons with different numbers of π bonds, where it is observed that the presence of π bonds generally increases the positron binding energies. These molecules were chosen because other global molecular parameters (e.g., polarizability, dipole moment, and geometry) are approximately constant, and so the observed differences in ε_B can be related to changes in the nature of the bonds. The molecular ionization potential E_i is an exception: for these molecules, the inclusion of π bonds tends to decrease E_i, and the number of π bonds also exhibits a correlation with ε_B. Comparison with other molecules with π bonds indicates that the changes in ε_B are better correlated with the changing electronic structure of the bonds rather than as a direct dependence of ε_B on E_i. The relationship between the dependence of ε_B on the number of π bonds and electron-positron correlation effects (such as virtual positronium formation) is discussed.

I. INTRODUCTION

To date, positron-molecule binding energies, ε_B, have been measured for over 90 molecules [1–5]. The data show that ε_B depends sensitively upon molecular composition and structure. However accurate theoretical predictions of ε_B continue to represent a major challenge. One significant issue is that the correlation potential can be much larger than the lowest order electrostatic terms. This includes not only the polarization terms but also the effects of virtual positronium, which is unique to positron-matter interactions [6–13]. It is often hard to obtain reliable results from simple calculations; and on the other hand, even for moderate size polyatomics, the computational cost for more sophisticated calculations can become quite high [9, 12–17]. Thus further experimental studies of selected sets of molecules can be of value as a guide to theory.

This paper describes studies of the dependence ε_B on the specific types of chemical bonds with a focus on π-bonded molecules. Molecules were chosen such that the electronic structure of the bonds can be changed while keeping the polarizability α, permanent dipole moment μ, and molecular geometry approximately fixed. Considered here are two remaining global parameters, the molecular ionization potential E_i and the number of π bonds in the molecule N_π.

New measurements are presented for hydrocarbon ring molecules with different numbers of π (i.e., 'double') bonds. The addition of each π bond, with the removal of two hydrogen atoms, results in only a slight change in the global α. In contrast, the change to the electronic structure associated with the π bond is significant, and for example, it often results in relatively large changes to E_i. Adding a π bond will also make the ring asymmetric, and this leads to a small permanent dipole moment. However, for all molecules considered, the change in μ is < 0.5 D, and in previous studies, this resulted in only a small change in ε_B, if any [1, 3, 18].

Since all of the new molecules studied are rings, the geometrical location of the atom cores is approximately the same while the number of π bonds is changed. Thus, it is argued here that the changes observed in the binding energies are due to the changing electronic structure of the bonds. These ring molecules are also compared with the results for other chemical species to elucidate the generality of the results. Although changes to E_i seem to be an indicator of changes in ε_B within a particular chemical series, the absolute value of E_i does not appear to be a useful parameter in predicting ε_B. Instead, it appears that *changes in* E_i are correlated with *changes in the number of* π *bonds* N_π, and both correlate with changes in ε_B.

The remainder of the paper is organized as follow. Section II briefly describes the experiments. Although the focus of this paper is on ε_B, the annihilation spectra are presented and briefly discussed. The ε_B results are discussed in Section III, where they are placed in context with data for other π-bonded molecules. Further, the results are related to other parametric studies [1, 4, 19] and to a new many-body calculation [13]. Section IV presents a summary and concluding remarks.

II. SPECTRAL MEASUREMENTS

Low-energy positron annihilation spectra for molecules often exhibit distinct peaks that are identified as vibrational Feshbach resonances (VFR) and associated with IR active vibrational modes (i.e., mediated by electric-dipole coupling) [22–24]. These resonances, located at energy ε_ν, are downshifted from the vibrational mode energy, $\hbar\omega_\nu$, by the positron-molecule binding energy, ε_B,

$$\varepsilon_\nu = \hbar\omega_\nu - \varepsilon_B. \tag{1}$$

* jrdanielson@ucsd.edu

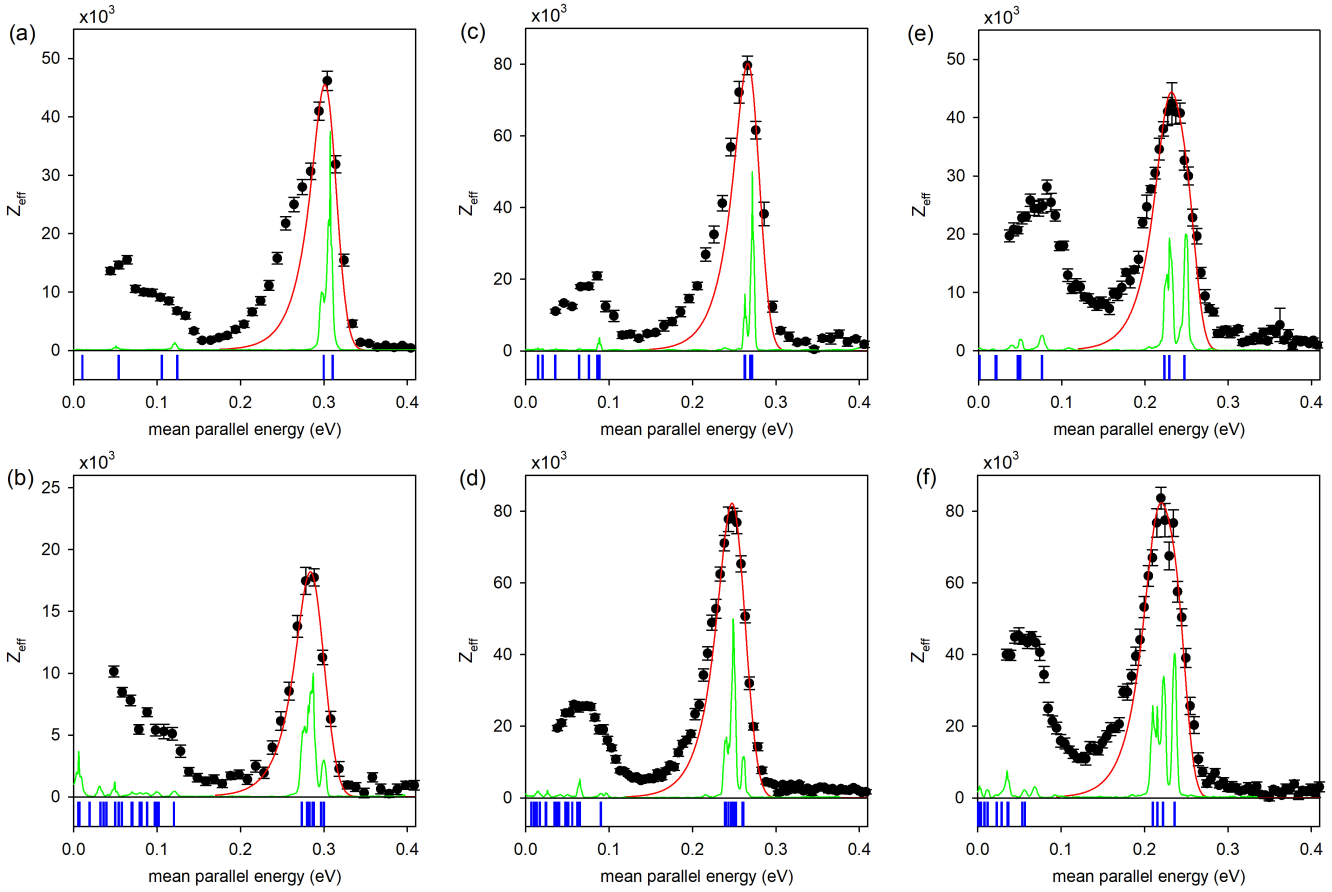

FIG. 1. Z_{eff} data plotted versus beam energy for (a) cyclopentane (ε_B = 49 meV), (b) cyclopentene (ε_B = 70 meV), (c) cyclohexane (ε_B = 82 meV), (d) cyclohexene (ε_B = 105 meV), (e) 1,4-cyclohexadiene (ε_B = 116 meV) and (f) 1,3-cyclohexadiene (ε_B = 132 meV). Error bars are statistical. Solid red line is the VFR fit to the high energy CH modes. Vertical lines show the locations of the downshifted IR-active fundamental vibrational modes. Solid green line is the arbitrary scaled, downshifted infrared spectrum [20].

Thus, if the vibrational mode energies are known, the locations of the resonances provide a direct measurement of the positron-molecule binding energy ε_B.

The experimental techniques to study these resonances have been described in detail previously [2, 23, 25]. Slow positrons ($\sim$ eV) are provided by a ^{22}Na radioisotope source and a solid neon moderator. They are magnetically guided into a three-stage buffer-gas trap [26]. The positrons are accumulated in a Penning-Malmberg trap and cooled to $\sim$ 300 K by collisions with N_2 and CF_4[27]. After cooling to the ambient temperature, the positrons are gently ejected from the trap by pulsing the confining electrodes to form a nearly monoenergetic positron beam [25], with the mean beam-transport energy of 0.7 eV and with a total energy spread $\leq$ 40 meV, FWHM. The typical number of positrons per pulse is $\sim 20,000$, but this can be varied depending upon the experiment.

The beam is magnetically guided into a gas cell where an electrode is electrically biased to set the mean parallel energy of the beam (i.e., the energy associated with the motion of the positrons in the direction of the magnetic field). The test gas is injected into the gas cell through a leak valve. The pressure range is maintained in the range $1-30$ μtorr (depending on the molecule and annihilation signal strength), as measured with a manometer. Single annihilation gamma rays are measured while the beam interacts with the test gas. The beam energy distribution is measured using a retarding potential analyzer (RPA) [2, 25, 28]. The count rate *vs* positron energy is converted into a normalized annihilation rate Z_{eff} [23] using the known number of positrons per pulse, the gas pressure, and the detector calibration.

Shown in Fig. 1 are the annihilation spectra for cyclopentane (C_5H_{10}), cyclopentene (C_5H_8), cyclohexane (C_6H_{12}), cyclohexene (C_6H_{10}), 1,4-cyclohexadiene (C_6H_8), and 1,3-cyclohexadiene (C_6H_8) as a function of the mean parallel energy of the positron beam. In the work presented here, mean parallel energy is used, since it can be measured directly using the RPA. The spectrum for benzene (C_6H_6) is presented in Fig. 2. The error bars for Z_{eff} are statistical based on the overall annihilation count rate. The energy scale is believed to be

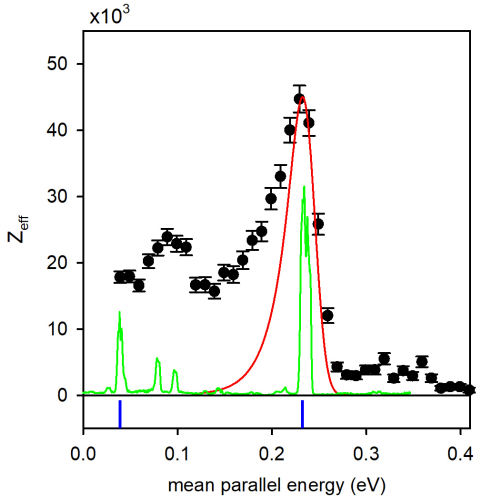

FIG. 2. $Z_{\rm eff}$ data plotted versus beam energy for benzene (ε_B = 133 meV). Error bars are statistical. Solid red line is the VFR fit to the high energy CH mode. Vertical lines show the locations of the downshifted IR-active fundamental vibrational modes. Solid green line is the arbitrary scaled, downshifted infrared spectrum [20]. This is a new measurement that updates the results presented in Ref. [21].

good to ±2 meV based on the reproducibility of measurements (e.g., separated by several months) and measurement of the time-of-flight of the positrons through the gas cell. Recently, we published high-resolution spectra for both cyclopentane [29] and benzene [30] using a cryotrap based beam (50K), and the measured values of ε_B are the same to within ±1 meV. However, to maintain consistency with the other measurements, only data using the 300 K beam are reported here.

The spectra in Fig. 1 all show distinct resonant structures with the most prominant peak in the energy range $0.2 - 0.3$ eV. These resonances are associated with the high-energy, dipole-allowed C-H stretch vibrational modes. The specific vibrational mode energies change depending on the types of bonds in each molecule. For example, the C-H stretch modes associated with carbons that participate in a double bond are typically higher in energy than the normal C-H stretch vibrations associated with methylene (CH_2) groups. The current BGT beam resolution (FWHM $\sim$ 36 meV) is not sufficient to separate these peaks. Thus, the total width of the resonance will depend on the spacing of the vibrational modes, and this leads to a broader resonant peak in molecules that exhibit a larger spread in mode energies. This needs to be accounted for in order to get the best fits to the resonances.

To fit to the measured C-H stretch peak, the resonances associated with the IR-active fundamental modes are treated as delta functions. They are convolved with the beam energy distribution and then summed to yield a single resonance peak. The total width of the resonance is a combination of the beam parameters and the spread of the vibrational modes. The binding energy and peak magnitude are independently scanned to obtain the best fit to the data, which then determines the experimental ε_B. The result is shown as the solid red line in each plot. For this study, only the IR active CH stretch modes have been used to obtain ε_B. No attempt has been made to fit the entire spectrum, although this could be investigated in the future. The downshifted locations of the IR-active vibrational modes used in the fit are shown in Fig. 1 (from [31–36]). The downshifted IR spectra (from Ref. [20], arbitrary amplitude scale) are also shown to indicate the contribution that the spread of mode energies may have to the resonance widths.

This fitting process was repeated for each molecule (solid red line), and the results are listed in Table 1 along with relevant global molecular parameters. As expected, the data show that the 6-carbon molecules (with larger α) have larger ε_B values than the 5-carbon molecules. However, there is a distinct increase in ε_B for the molecules with π bonds. This increase in ε_B is also correlated with a decrease in $E_{\rm i}$. The last two columns show that, for all the molecules except benzene, there is a strong correlation between the number of π bonds, N_π, and $E_{\rm i}$. The question then becomes whether it is the changing electronic structure of the bonds or the changing ionization energy that is responsible for the increased ε_B.

As shown in Figs. 1 and 2, the fits provide a good description of the peaks in most molecules. However, some of the molecules exhibit a slight excess broadening on the low energy side of the C-H peak. The most extreme examples are cyclopentane in Fig. 1(a) and benzene in Fig. 2, although this is also apparent in cyclohexane, Fig. 1(c). These features are discussed in more detail below. In all cases, the analyses shown by the red curves in Figs. 1 and 2 were used, since the high energy sides of the resonances are well fit. With the exception of cyclohexane and benzene, both sides of the peaks are reasonably well fit, and the binding energy is tightly constrained (i.e., with a total uncertainty of $\pm\ 3 - 5$ meV).

III. DISCUSSION

The values of ε_B from Figs. 1 and 2 and other relevant parameters are summarized in Table I. The global molecular parameters (α, μ, $E_{\rm i}$, N_π) are used to group ε_B for the different molecules, and trends in the data are used to clarify the important factors determining ε_B. The goal is not to find a new empirical fit (e.g., with different and/or more fit parameters), but rather to better understand the role of π bonds in determining ε_B.

Data for set of comparison molecules are given in Table II. This group includes chain alkanes [18, 21], ethylene [23], chloro-substituted methanes [4, 38], and chloro-substituted ethylenes [4, 39]. The ethylenes all have a single C-C associated π bond, and so they form a good set to compare to the new measurements. In contrast to the ring molecules, the chloro-substituted molecules of-

TABLE I. Fit results and molecular parameters for ring hydrocarbons with different numbers of π bonds. All data taken with room temperature positron beam, $\sigma_{||} \approx 10$ meV, $\sigma_{\perp} \approx 20$ meV. Values for α, μ, and $E_{\rm i}$ from [37]. ε_{pk} is the energy for the peak of the resonance and $Z_{\rm eff}(\varepsilon_{pk})$ is the value of $Z_{\rm eff}$ at the peak. Symbols identify the number of carbons, solid symbols have one or more π bonds, hollow symbols have no π bonds. Superscript A indicates that the π bonds are aromatic.

Molecule	Formula	Symbol	ε_B [meV]	ε_{pk} [eV]	$Z_{\rm eff}(\varepsilon_{pk})$	α [10^{-30}m^3]	μ [D]	$E_{\rm i}$ [eV]	N_π
cyclopentane	C_5H_{10}	□	49 ± 3	0.303	46,200	9.1	0	10.3	0
cyclopentene	C_5H_8	■	70 ± 3	0.284	18,000	8.9	0.2	9.0	1
cyclohexane	C_6H_{12}	◇	82 ± 5	0.265	80,200	11.0	0	9.9	0
cyclohexene	C_6H_{10}	◆	105 ± 3	0.247	81,600	10.7	0.33	9.0	1
1,4-cyclohexadiene	C_6H_8	◆	116 ± 4	0.233	44,000	11.0	0	8.8	2
1,3-cyclohexadiene	C_6H_8	◆	132 ± 3	0.222	81,800	10.6	0.44	8.3	2
benzene (aromatic)	C_6H_6	◆	133 ± 5	0.230	44,700	10.4	0	9.3	3^A

TABLE II. Binding energy data and molecular parameters for comparison molecules. Values for α, μ, and $E_{\rm i}$ from [37]. Chloro-molecule measurements from [4]. The ε_B values for ethane and ethylene are older measurements [23] and have larger error bars. Solid symbols have one or more π bonds, hollow symbols have no π bonds.

Molecule	Form.	Sym.	ε_B [meV]	α [Å^3]	μ [D]	$E_{\rm i}$ [eV]	N_π
cl.methane	CH_3Cl	○	26 ±6	4.4	1.9	11.2	0
dicl.methane	CH_2Cl_2	○	32 ±4	6.5	1.6	11.3	0
chloroform	$CHCl_3$	○	37 ±3	8.4	1.0	11.4	0
carb.tet.	CCl_4	○	55 ±8	10.5	0.0	11.5	0
1,2-trans-DCE	$C_2H_2Cl_2$	●	14 ±3	8.2	0.0	9.6	1
1,2-cis-DCE	$C_2H_2Cl_2$	●	66 ±8	8.0	1.9	9.7	1
1,1-DCE	$C_2H_2Cl_2$	●	30 ±5	8.1	1.3	9.8	1
tri-CE	C_2HCl_3	●	50 ±6	10.0	0.8	9.5	1
tetra-CE	C_2Cl_4	●	57 ±6	12.0	0.0	9.3	1
ethane	C_2H_6	▽	2 ±5	4.4	0.0	11.5	0
ethylene	C_2H_4	▼	20 ±8	4.2	0.0	10.5	1

ten have a significant permanent dipole moment unless it happens to be zero by symmetry. Thus, the chloromethanes are included as a control group, since they lack a double-bond, but otherwise have comparable α and μ to the chloro-ethylenes. Recently, there was a combined theoretical and experimental study of chloro-substituted molecules, including the molecules considered here [4]. Generally, the modeling showed good agreement with the measurements except for the chloro-ethylenes (discussed below).

The measured ε_B for the comparison molecules and the associated molecular parameters are shown in Table. II. These molecules are compared to the new measurements in Figs. 3(a) - 3(d), as a function of polarizability α, dipole moment μ, ionization potential $E_{\rm i}$, and number of π bonds N_π, respectively. In the figures, all of the filled data symbols have 1 or more π bonds, whereas the open symbols have none.

A. Polarizability and dipole moment

The molecular polarizability is dominated by the carbon and halogen atoms [40], with the change in the number of hydrogen atoms making only a small difference. This is best seen by comparing cyclohexane and benzene, where the loss of the six hydrogen atoms only reduces α by $\sim 5\%$, and so the non-saturated and saturated rings have about the same α values. Further, exchanging a carbon for a chlorine atom also keeps α approximately unchanged. For example, chloroform with one carbon and three chlorines has about the same α as dichloroethylene with two carbons and two chlorines. Thus, the plot of ε_B *vs* α as shown in Fig. 3(a), results in groups of approximately constant α.

The most general statement is that typically ε_B increases with α. This is best exemplified in Fig. 3(a) by the approximately linear increase of the chain alkanes (open triangles) with α [18, 23]. This roughly holds for the other molecules as well, although there is a significant spread. The new rings molecules (squares and diamonds) all show increased ε_B relative to the alkane line. In contrast, the chloro-substituted molecules are observed to spread both above and below this line.

For both the ring molecules and the alkane chains considered here, the dipole moment is either zero or very small (< 0.5 D). As noted above, the addition of the π bonds does not add a significant dipole moment. In contrast, the chloro-substituted molecules have dipole moments typically between $1 - 2$ D, except for those that are zero by symmetry. Typically, larger dipole moments tend to enhance the binding energy. However, for those cases the overall geometry of the molecule is also important (e.g. see [4, 5, 18]), and thus there appears to be no simple predictive relationship using just these parameters.

B. Ionization potential and number of π bonds

The ionization potential of the molecule is set by the energy of the highest occupied molecular orbital (HOMO). For positron interactions, this also determines the positronium (Ps) formation threshold, $E_{\rm i} - 6.8$ eV,

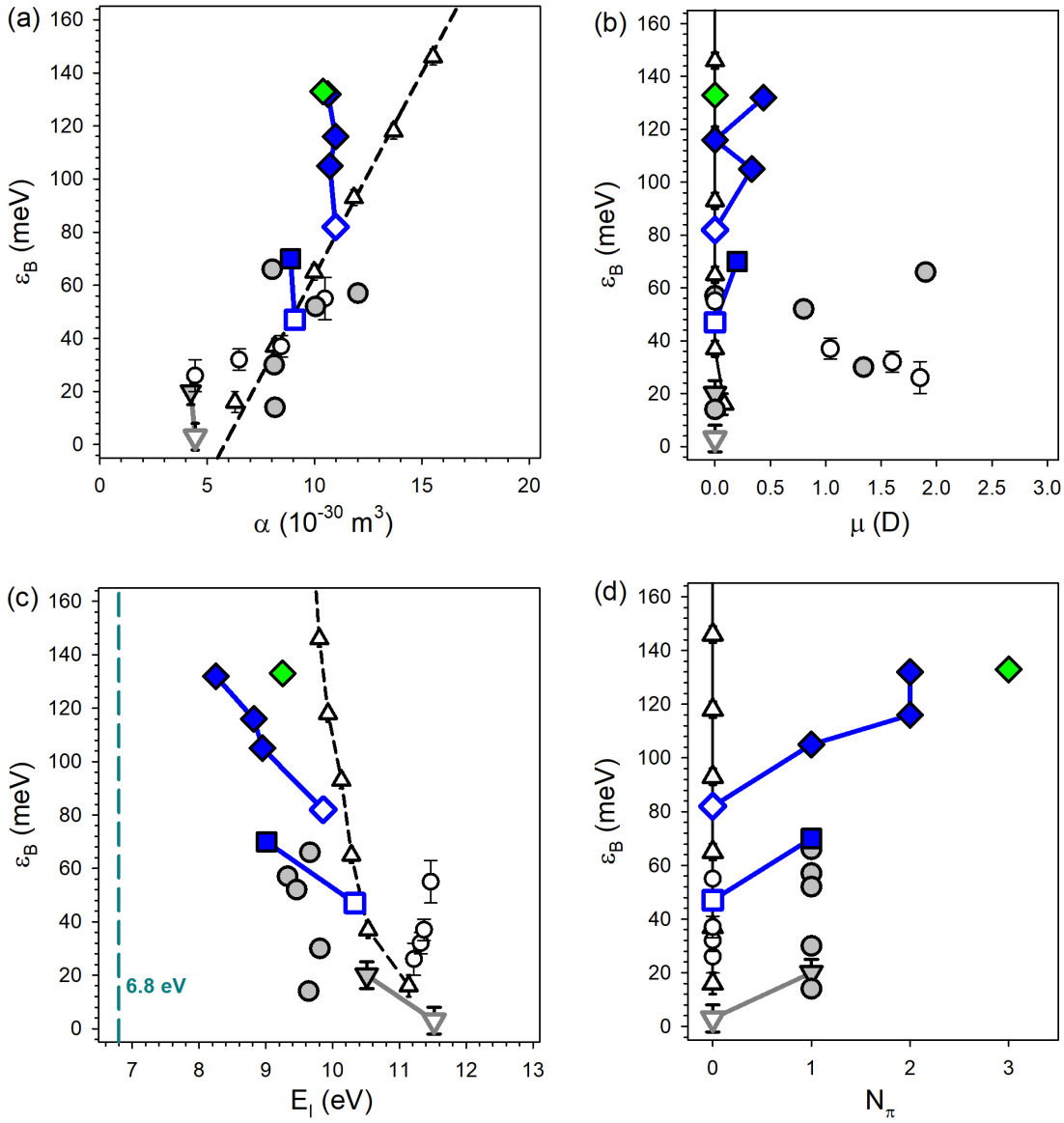

FIG. 3. Measured positron binding energy, ε_B, vs. molecular parameters (a) α, (b) μ, (c) E_i, and (d) N_π. Up-triangles are chain alkanes, squares are 5-carbon rings, diamonds are 6-carbon rings, down-triangles are ethane and ethylene, circles are chloro-substituted methanes and ethylenes. Solid symbols have 1 or more π bonds, hollow symbols have zero π bonds. Dashed lines show the trend for the chain-alkanes. Solid lines are guides to the eye that connect molecules with same number of carbon atoms. For other details, see Tables 1 and 2.

where 6.8 eV is the binding energy of the ground state of Ps [41]. It is expected that the effect of "virtual positronium" can increase the strength of the attractive part of the correlation energy and lead to larger binding energies for targets with low E_i. This is similar to what has been calculated for positron-atom binding [8]. Early attempts to do this for molecules were inconclusive [1]. However recently, there was published a machine-learning study that appeared to identify such a dependence of ε_B on E_i [19].

The ring molecules for which data are shown in Figs. 1 and 2 provide a good opportunity to explore this effect further. As noted above, the addition of π bonds does not change α or μ appreciably, and thus the observed changes can be assumed to be due to the different electronic structures of the bonds. One global parameter that does change appreciably is E_i; namely, as shown in Table I, the addition of π bonds almost always lowers E_i. This also correlates with larger ε_B relative the rings with no π bonds [i.e., hollow square and diamond in Fig. 3(c)].

The key question is whether it is E_i or some other property of the π bonds that leads to the enhanced values

of ε_B. Shown in Fig. 3(d) is a plot of ε_B as a function of N_π. It is striking that this plot is roughly a mirror image of Fig. 3(c), which plots ε_B *vs.* E_i. Thus, it appears that the number of π bonds is also a relevant parameter. This was used in an early parameterization of the ε_B data [1], where it was seen that, in order to fit the aromatic molecules benzene and naphthalene, a term linear in N_π was required.

Beyond the new data for ring molecules, there are several other interesting features in Figs. 3(c) and 3(d). Comparing ethane to ethylene (down triangles), there is a similar drop in E_i and an increase in ε_B for the molecule with the π bond (ethylene). As can be seen in both plots, the increase $\Delta\varepsilon_B \sim 20$ meV from ethane to ethylene is approximately the same as the increase from cyclopentane to cyclopentene, and from cyclohexane to cyclohexene. However, it is clear that the *absolute values of* E_i are quite different for these molecules, and so this argues against a direct dependence of ε_B on E_i.

A more extreme example is the comparison of the chloro-methanes (hollow circles) to the chloro-ethylenes (solid circles) in Figs. 3(c) and (d). Unlike the rings, the geometric shape of these molecules does change considerably from one group to the other. This leads to significant variation in the resulting dipole moments, making the comparison more difficult than for the case of the rings. However, both groups have the same types of atoms (carbon, hydrogen, and chlorine), the molecules are comparable in size (5 *vs* 6 total atoms), and they have comparable spreads in α and μ (Figs. 3(a),(b)). Thus, although it would not be appropriate to compare individual molecules, it is reasonable to compare members (or subsets) of the respective groups. Looking at Fig. 3(c), a grouping *vs* E_i is apparent, where the chloro-ethylenes, each with a single π bond, have lower E_i by ~ 2 eV relative to the chloro-methanes. Even with this large gap, the two sets of molecules exhibit about the same spread in ε_B. So, for this case, the addition of π bonds does not appear to increase ε_B. Similarly, the smaller *absolute value of* E_i appears to make no significant change in ε_B.

The data for benzene [i.e., green diamond in Fig. 3(c)] is an exception. With three π bonds, it would normally be expected to lower E_i even further. However, as is well known, benzene is aromatic, where the π bonds form a more stable, lower-energy electronic structure, and thus the ionization energy actually rises slightly. If there was a direct dependence on E_i one might then expect ε_B to drop. However, as seen in the data, ε_B is still larger than 1,4-cyclohexadiene and comparable to 1,3-cyclohexadiene. Here again, it appears that the absolute value of E_i alone cannot explain the enhancement of ε_B.

The dependence of ε_B on molecular composition and geometry was considered recently in a study of chlorine-substituted molecules, including those considered here [4]. In that work, a model correlation potential was used with the full molecular geometry in order to calculate ε_B. These calculations fit several parameters to one or more molecules in order to tune the model. Once tuned, the model can be used for a wide range of molecules with similar substitutions. This was shown to work quite well for the broad range of chlorine-substituted molecules, including the chloro-methanes, chloro-propanes and other molecules with no π bonds. It was also tested with ethylene and the chloro-ethylenes. For ethylene, the model yielded a value of ε_B a factor of four *s*maller than that of the measurement.

For the chloro-ethylenes, the calculations were systematically *l*arger by as much as a factor of two. The model used the same parameters as for the other molecules, and so the only difference was the presence of the π bond. Thus, something more would be needed to model these effects (i.e., similar to the conclusion of [1]). It is interesting to note that it would have to lead to a *decrease* in ε_B for chloro-ethylenes, and an *increase* in ε_B for ethylene. This is in contrast to the ring hydrocarbons and ethylene, where the effect of the π bonds is always to increase ε_B. This effect can also be seen in Fig. 3(a), where several chloro-ethylenes are seen to be *below* the linear alkane curve.

As a summary statement, albeit approximate, there is a correlation, not between E_i and ε_B, but between *changes in* E_i and the *changes in* ε_B for similar molecules. A roughly equivalent (still approximate) parameterization can be made with the number of π bonds, N_π.

Additional theoretical insights into the roles of E_i and N_π in determining ε_B come from the recent *ab initio* many-body calculations of Hofierka et al. [13]. They are able to include virtual positronium in a systematic manner in the correlation potential and show that it can lead to factors of two or more increase in ε_B. They also show that increases in ε_B do not correlate with the absolute E_i, rather the increase is due to the sum of the interactions with many valence electronic orbitals. In fact, for several molecules, the HOMO (which determines E_i) actually contributes *l*ess than do some of the more deeply bound electronic orbitals.

The prominent role of π bonds in positron-molecule attraction is likely due to the fact that the positrons are repelled by the positivley charged atomic cores. Electrons that form σ (single) bonds are generally found between the nuclei, while the electrons in π bonds are located away from the line (or plane, as in ethylene or benzene) that contains the atomic cores. Thus, it is "easier" for positrons to access the electron-rich regions of the π bonds, as compared with the σ bonds. The electrons in π bonds effectively contribute more to the positron attraction, as compared with electrons in the σ bonds, while their other contributions (e.g., to the polarizability) are approximately the same.

C. Other features of the annihilation spectra

There are additional features of the annihilation spectra shown in Figs. 1 and 2 that are worthy of note. Returning to the feature observed on the low-energy side of

the CH stretch peaks, the spectra of both cyclopentane [29] and benzene [30], studied with the higher-resolution cryogenic trap-based beam, begin to resolve small peaks at these locations. They may be related to combination vibrations near these locations that are visible in the IR spectrum.

The magnitudes of the $Z_{\rm eff}$ spectra also show interesting trends. Not surprisingly, the spectral magnitude for the five carbon rings (cyclopentane and cyclopentene) are smaller than the six carbon rings. This is consistent with the scaling with molecular size seen for other alkanes and similar hydrocarbons. However, cyclopentene is a factor of ~ 2 *smaller* than cylopentane, even though cyclopentene nominally has more IR active modes due to lower symmetry (C2v vs D5h). However, the integrated-IR for cylopentane is 50% larger, and since the symmetries are only approximate [42, 43], the larger activity made lead to more resonances. In any case, the $Z_{\rm eff}$ values for these molecules are enhanced above simple expectations [2, 24], and so some level of intramolecular vibrational redistribution (IVR) is likely occurring [44–46]. On the other hand, the infrared study of the CH modes of hydrocarbons by Stewart and McDonald found that the dilution factor for the two molecules was comparable (i.e., from which one would expect comparable levels of enhancement) [47]. Thus the origin of the relative magnitudes of $Z_{\rm eff}$ for cyclopentane and cyclopentene remains an open question.

In contrast to cyclopentane and cyclopentene, the six-carbon molecules cyclohexane and cyclohexene have comparable annihilation magnitudes, and 1,3-cyclohexadiene is also about the same in magnitude. Although these molecules are structurally similar, given the different symmetries, it would be surprising if they had the same vibrational mode densities, and so it it is surprising that $Z_{\rm eff}$ is the same for all three. The last two 6-carbon rings, 1,4-cyclohexadiene and benzene, are both about a factor of two smaller. The symmetries of the two are different as are the number of IR active modes, again leading to a surprising result. However, to make quantitative comparisons will require detailed calculations of the dipole coupling strengths and the density of vibrational states for the modes in these molecules.

IV. SUMMARY AND CONCLUDING REMARKS

Presented here are annihilation spectra for ring hydrocarbons with different numbers of π bonds. The resulting measurements of ε_B were summarized in Table 1, along with selected molecular parameters. Rings were chosen because the electronic structure of the bonds could be changed while leaving most global molecular parameters approximately fixed, thus allowing for a better separation of bond effects. A large effect of the π bonds is to decrease the molecular ionization potential, and there is also some correlation with positron-molecule binding energies with the types of molecular bonds. However, the measurement for benzene, which has a higher $E_{\rm i}$ and a large ε_B, and for the chloro-ethylenes with lower $E_{\rm i}$ and smaller ε_B, suggest that the correlation is likely more related to the strength of the positron interaction with the bond electrons, rather than directly linked to the absolute $E_{\rm i}$, although both effects could be occurring. One might speculate that the chlorine atoms perturb the π bonds such that the orbitals are different than in the rings, even though $E_{\rm i}$ is also reduced. It may also be that the larger core size of the chlorine atom results in pushing the positron wavefunction farther away, thus limiting the interaction with the bond and subsequently reducing ε_B. Both of these consideration would argue that it is the nature of the bond that matters most in the interaction with the positron.

These experimental data and the interpretation presented here were also discussed in the context of the results of the recent many-body theory of Hofierka et al. [13]. In particular their calculation included the important effect of virtual positronium in enhancing ε_B. Relevant to the current discussion, their calculations for molecules with π bonds demonstrated a strong dependence on the molecular orbitals and showed that the strongest interaction is often not necessarily with the orbital that sets $E_{\rm i}$. Thus absolute $E_{\rm i}$ will not necessarily be the parameter that sets ε_B. Rather it is the structure of the electronic orbitals and how they interact with the positron that dominates the correlation interaction.

Evidence, from the experiments, model-potential calculations and many-body theory, support the idea that the nature of the bonds has an important contribution that goes beyond what is seen in the global parameters. This does not mean that simple relationships cannot be found amongst particular molecular series. It is clear these relationships do exist when the interactions are similar, the best example being the saturated alkane chains. Instead, as with geometry, the electronic structure of the bond is another important parameter that needs to be considered, and whose effects are not always proportional to the changes in global parameters. Due to these less direct relationships, a formula for molecules with one type of bond will not likely be transferable to molecules with different bonds, regardless of the similarity of other global molecular parameters.

ACKNOWLEDGMENTS

We would like to thank Gleb Gribakin, Andrew Swann, and Dermot Green for many helpful comments and suggestions related to the current work. This work was supported by the U. S. NSF, grant PHY-2010699.

[1] J. R. Danielson, J. A. Young, and C. M. Surko, J. Phys. B **47**, 225209 (2009).
[2] G. F. Gribakin, J. A. Young, and C. M. Surko, Rev. Mod. Phys. **82**, 2557 (2010).
[3] J. R. Danielson, A. C. L. Jones, J. J. Gosselin, M. R. Natisin, and C. M. Surko, Phys. Rev. A **85**, 022709 (2012).
[4] A. R. Swann, G. F. Gribakin, J. R. Danielson, S. Ghosh, M. R. Natisin, and C. M. Surko, Phys. Rev. A **104**, 012813 (2021).
[5] J. R. Danielson, S. Ghosh, and C. M. Surko, J. Phys. B **54**, 225201 (2021).
[6] V. A. Dzuba, V. V. Flambaum, G. F. Gribakin, and W. A. King, Phys. Rev. A **52**, 4541 (1995).
[7] D. M. Schrader, NIM:B **143**, 209 (1998).
[8] J. Mitroy, M. W. Bromley, and G. G. Ryzhikh, J. Phys. B **35**, R81 (2002).
[9] M. Tachikawa, I. Shimamura, R. Buenker, and M. Kimura, Nuclear Instruments and Methods in Physics Research Section B: Beam Interactions with Materials and Atoms **192**, 40 (2002).
[10] G. F. Gribakin and J. Ludlow, Phys. Rev. A **70**, 032720 (2004).
[11] J. Mitroy, Phys. Rev. A **72**, 062707 (2005).
[12] M. Tachikawa, Y. Kita, and R. J. Buenker, Physical Chemistry Chemical Physics **13**, 2701 (2011).
[13] J. Hofierka, B. Cunningham, C. M. Rawlins, C. H. Patterson, and D. G. Green, Nature **606**, 688 (2022).
[14] H. A. Kurtz and K. D. Jordan, J. Chem. Phys. **75**, 1876 (1981).
[15] H. Chojnacki and K. Strasburger, Molecular Physics **104**, 2273 (2006).
[16] M. Tachikawa, Y. Kita, and R. J. Buenker, New Journal of Physics **14**, 035004 (2012).
[17] K. Koyanagi, Y. Kita, and M. Tachikawa, The European Physical Journal D **66**, 1 (2012).
[18] A. R. Swann and G. F. Gribakin, J. Chem. Phys. **153**, 184311 (2020).
[19] P. H. R. Amaral and J. R. Mohallem, Phys. Rev. A **102**, 052808 (2020).
[20] d. NIST Mass Spectrometry Data Center, William E. Wallace, in *NIST Chemistry WebBook, NIST Standard Reference Database Number 69*, edited by P. J. instrom and W. G. Mallard (National Institute of Standards and Technology, Gaithersburg MD, 20899) Chap. Infrared Spectra.
[21] J. A. Young and C. M. Surko, Physical Review A **77**, 052704 (2008).
[22] S. J. Gilbert, L. D. Barnes, J. P. Sullivan, and C. M. Surko, Physical Review Letters **88**, 043201 (2002).
[23] L. D. Barnes, S. J. Gilbert, and C. M. Surko, Phys. Rev. A **67**, 032706 (2003).
[24] G. F. Gribakin and C. M. R. Lee, Phys. Rev. Lett. **97**, 193201 (2006).
[25] M. R. Natisin, J. R. Danielson, and C. M. Surko, Phys. Plasmas **23**, 023505 (2016).
[26] T. J. Murphy and C. M. Surko, Phys. Rev. A **46**, 5696 (1992).
[27] J. R. Danielson, D. H. E. Dubin, R. G. Greaves, and C. M. Surko, Rev. Mod. Phys. **87**, 247 (2015).
[28] S. Ghosh, J. R. Danielson, and C. M. Surko, J. Phys. B **53**, 085701 (2020).
[29] S. Ghosh, J. R. Danielson, and C. M. Surko, Phys. Rev. Lett. **125**, 173401 (2020).
[30] S. Ghosh, J. R. Danielson, and C. M. Surko, submitted for publication (2022).
[31] L. M. Sverdlov, M. A. Kovner, and E. P. Krainov, "Vibrational spectra of polyatomic molecules,(israel program for scientific translations)," (1974).
[32] T. Shimanouchi *et al.*, *Tables of molecular vibrational frequencies*, Vol. 1 (National Bureau of Standards Washington, DC, 1972).
[33] N. Neto, C. Di Lauro, E. Castellucci, and S. Califano, Spectrochimica Acta Part A: Molecular Spectroscopy **23**, 1763 (1967).
[34] C. Di Lauro, N. Neto, and S. Califano, Journal of Molecular Structure **3**, 219 (1969).
[35] H. D. Stidham, Spectrochimica Acta **21**, 23 (1965).
[36] S. N. Thakur, L. Goodman, and A. G. Ozkabak, J. Chem. Phys. **84**, 6642 (1986).
[37] D. R. Lide, ed., *CRC Handbook of Chemistry and Physics*, 89th ed. (CRC Press, 2008-2009).
[38] A. C. L. Jones, J. R. Danielson, M. R. Natisin, C. M. Surko, and G. F. Gribakin, Phys. Rev. Lett. **108**, 093201 (2012).
[39] M. R. Natisin, J. R. Danielson, G. F. Gribakin, A. R. Swann, and C. M. Surko, Physical Review Letters **119**, 113402 (2017).
[40] K. J. Miller, Journal of the American Chemical Society **112**, 8533 (1990).
[41] M. Charlton, J. W. Humberston, and J. W. Humberston, *Positron physics*, Vol. 11 (Cambridge university press, 2001).
[42] I. M. Milla, Molecular Physics **20**, 127 (1971).
[43] E. J. Ocola, L. E. Bauman, and J. Laane, J. Phys. Chem A **115**, 6531 (2011).
[44] G. F. Gribakin and C. M. R. Lee, Eur. Phys. J. D **51**, 51 (2009).
[45] J. R. Danielson, A. C. L. Jones, M. R. Natisin, and C. M. Surko, Phys. Rev. A **88**, 062702 (2013).
[46] G. F. Gribakin, J. F. Stanton, J. R. Danielson, M. R. Natisin, and C. M. Surko, Phys. Rev. A **96**, 062709 (2017).
[47] G. M. Stewart and J. D. McDonald, J. Chem. Phys. **78**, 3097 (1983).